AIMS Energy, 11(1): 171–196.
DOI: 10.3934/energy.2023010
Received: 04 October 2022
Revised: 18 February 2023
Accepted: 20 February 2023
Published: 02 March 2023

http://www.aimspress.com/journal/energy

Research article

Optimum configuration of a dispatchable hybrid renewable energy plant using artificial neural networks: Case study of Ras Ghareb, Egypt

Mohamed Hamdi*, Hafez A. El Salmawy and Reda Ragab

Mechanical Power Engineering Department, Faculty of Engineering, Zagazig University, Zagazig 44519, Egypt

* **Correspondence:** Email: Mohamedhamdi4474@gmail.com, mhamdyi@zu.edu.eg; Tel: +20 1005482064.

Abstract: The present paper examines the potential hybridization for a dispatchable hybrid renewable energy system (HRES). The plant has been examined for existence in the city of Ras Ghareb, Egypt and follows the load profile of Egypt. The proposed plant configuration contains a wind plant, a solar photovoltaic plant, vanadium redox flow batteries (VRFBs) and a hydrogen system consisting of an electrolyzer, hydrogen tanks and fuel cells (FCs), the latter of which are for both daily and seasonal storage. Professional software tools have been used to model the wind and solar resources. Simulations for both the battery and hydrogen generation and electrolyzer operation are also considered. The output of these simulations is used to configure the HRES using MATLAB. The optimization objective function of the HRES is based on the least levelized cost of energy (LCOE) with constraints for a zero loss of power supply probability (LPSP) and curtailed energy. The optimization has been achieved by using artificial neural networks and a MATLAB program. The results show that the optimal system can handle 91.2% of the load directly from the renewable energy sources (wind and solar), while the rest of the demand comes from the storage system (FCs and VRFBs). The LCOE of the optimal system configuration is (USD) 9.3 ¢/kWh, with both the LPSP and curtailed energy at zero values. This cost can be reduced by 14.5% if the constraint of zero curtailed energy is relaxed by 10%. Despite the load being maximum in summer, the energy storage requirement is predicted to be maximum in winter due to the low wind profile and solar radiation in winter months. Energy storage system size is dependent on both seasonal and daily variations in wind and solar profiles. In addition, energy storage size is the main factor that determines the LCOE of the system.

Keywords: hybrid renewable energy systems; dispatchable power plant; wind energy; solar energy; energy storage; ANN

Abbreviations: ABC: Artificial bee colony; N: Project lifetime; AEP: Annual energy production; OPEX: Operating expenses; ANN: Artificial neural network; PEM: Proton exchange membrane; Capex: Capital expenditures; PSO: Particle swarm optimizations; CRF: Capital recovery factor; PV: Photovoltaic; CSP: Concentrated solar power; RES: Renewable energy sources; D: Discount rate; SAM: System advisor model (NREL); DC: Direct current; SoC: State of charge (SOC = 1 at full charge); FC: Fuel cell; SOE: Solid oxide electrolyze; FOM: Annual discounted and inflated O&M; TC: Total cost; HRES: Hybrid renewable energy system; TPL: Total power Losses; I: Inflation rate; VRFB: Vanadium redox flow battery; IEA: International energy agency; WT: Wind turbine; LCC: Life cycle cost; LCoE: Levelized cost of energy; LLP: Loss of load probability; LPSP: Loss of power supply probability

1. Introduction

Renewable energy generation has remarkably increased worldwide, primarily due to the global greenhouse gas emission reduction targets and climate change slowdown goals. As the development of renewable energy plays a crucial role in the green economy, countries should start planning their energy policy to depend entirely on renewables [1–4]. According to the 2022 International Energy Agency (IEA) renewable energy market update, global renewable additions reached a new record of 295 GW per year [5]. According to IEA statistics, the share of renewable energy in the world's power production has climbed from 1.95% to 8.3% over the past 10 years (excluding hydropower) [6]. Introducing high levels of intermittent renewable resources in traditional power systems could have a negative impact on the system [7]. This may include a requirement of a balanced reserve [8], a curtailment of renewable electricity [9] and compromise on the reliability of thermal units exposed to high cycling rates due to the high penetration of renewable energy sources (RESs) [10].

RESs represent a significant alternative energy source; however, there is considerable concern regarding their dependence on unpredictable factors like wind speed and solar radiation. As a result of their unpredictability, individual energy sources are unable to supply a steady flow of electricity to meet the continuous demand. However, RESs can be integrated along with storage systems to supply the load with high reliability and predictability. Hybrid renewable energy systems (HRESs) can operate in a grid connected system or as isolated systems [11–13]. The simplest form of hybridization is the combination of wind and solar resources in consideration of the complementarity nature in their generation profiles. The literature is rich in examples of such hybrid systems with many different combinations of renewable sources. For instance, Al-Ghussain et al. [14] assessed the use of hybrid photovoltaic (PV)/wind plant to meet the demand of a cement factory. The results show that using a hybrid PV/wind plant met the demand of the plant with a levelized cost of energy (LCOE) that is less than the grid tariff. Storage technologies improve the hybrid system’s reliability, as it helps to decrease the loss of power supply and unmet load. Several storage technologies can be used in different hybrid

systems depending on the advantages and disadvantages of each technology. Table 1 lists common storage technologies used in hybrid plants, along with their citations in the literature.

Table 1. List of common storage technologies used in HRESs.

Renewables	Storage technology	Application	Ref.
PV	Batteries (Lead-acid, Li-ion, VRFB)	Grid-Connected	[15]
PV/Wind	Batteries (Lead-acid, Li-ion, VRFB)	Grid-Connected	[16,17]
PV/Wind	Batteries	Off-Grid	[18]
PV/Wind	Batteries/FC	Off-Grid	[19–21]
PV	Batteries/FC	Off-Grid	[22]
CSP/PV	Thermal/Batteries	Grid-Connected	[23]
PV/Wind	Batteries/FC	Off-Grid	[24]
PV	Batteries/Supercapacitor	Grid-Connected	[25]
PV	Fuel cell/Supercapacitor	Off-Grid	[26]
PV	Hydro storage	Grid-connected	[27]
PV/Biomass	FC	Off-Grid	[28]
PV/Diesel	Batteries	Off-Grid	[29,30]

From previous studies, it could be noticed that wind is less favorable than PV energy. This is due to the highly unpredictable nature of wind, as well as the sophisticated nature of the development of wind projects and the limited number of economically viable windy sites. In addition, the availability of dependable long-term wind speed data is another barrier. Most studies tend to assess off-grid systems, despite the need for HRES grid-connected systems to enhance the grid reliability.

Sizing an HRES is more complicated than sizing a single-source renewable system because of the characteristics of renewable energy resources, stochastic load demand and the large number of variables and parameters considered during the design of HREs. An optimum sizing strategy can help to reduce these issues while locating the lowest investment and maximizing the use of the system components. In the literature, numerous optimization approaches and tools have been widely published. Table 2 summarizes the most common optimization techniques used in HRES modeling.

Table 2. List of simulation techniques used in HRESs optimization.

HRES	Optimization technique	Constraints	Ref.
PV/Wind/Batteries	Genetic Algorithm	LPSP/LCOE	[31]
PV/Batteries/Diesel	Genetic Algorithm	LLP/LCOE	[32]
PV/Wind/FC	ABC	TPL/LCOE/Emissions	[21]
PV/Wind/FC/Micro-turbines	Fuzzy Logic	Energy Management	[33]
PV/Wind/FC/Solar thermal collector	PSO	Total cost	[34]
PV/Wind/Diesel/Batteries	Homer	LCOE	[35]
PV/Wind/Batteries/FC	Simulated Annealing	LCC	[36]

The human brain learning mechanism is used by artificial neural networks (ANNs), which can form an input-output connection for linear and nonlinear systems with little computational effort. Several studies have emphasized the application of ANNs for energy production prediction and weather forecasting. Brekken et al. [37] employed several methods to determine the appropriate size and control methodology of a zinc-bromine flow battery that would enhance the predictability of wind power production. Using ANN methodology resulted in the lowest energy cost among the other used techniques. Zhang et al. [38] introduced a hybrid optimization approach for PV/WT/hydrogen system sizing and employed ANNs in their weather forecasting. Their results suggest that a PV/hydrogen

combination is the cost-effective option. The authors of the current work presented a soft coupling between professional modeling software tools and ANNs to find the optimum configuration of a baseload HRES. Their results show that the LCOE is highly dependent on the storage system size [39]. A comprehensive review of the ANN utilization in HRESs is provided in [40]. From the literature, all usage of ANNs in HRESs is mainly for weather data prediction.

According to the previous studies, most of the previous research aimed to provide renewable generation for isolated systems, despite the fact that HRESs can also be used for dispatchable grid-connected systems. This concept has not yet been studied on a large scale. Also, utilizing two storage techniques to consider the daily and seasonal variation of renewable energy systems was rarely found in the literature. Furthermore, the coupling between professional resource assessment tools and artificial intelligence sizing techniques is almost absent.

The current work is a continuation of a persistent effort by the authors to employ an HRES as a utility grid-connected plant. An HRES consisting of PV/wind/battery/fuel cell (FC) has been simulated by using a variety of professional software tools. A storage dispatch method is adopted, with redox flow batteries serving as a daily storage system and molten carbon FCs purposed for seasonal storage. To achieve precise detailed output from the plant, each component of the HRES was optimally designed by using specialized professional software tools. WindPRO and WAsP are used to optimize the wind farm, and NREL system advisor model (SAM) software is used to optimize the PV farm, as well as simulations for both the battery hydrogen/FC systems. The objective is to optimally size a hybrid system that has been designed to serve as a dispatchable load plant, supplying the grid with a consistent load throughout the year at the lowest possible cost of power, considering hourly load throughout the year. The current work utilizes an ANN to enable discrete optimization through the generation of millions of cases to be assessed. The objective function is purposed to minimize the LCOE and curtailed (residual) energy while keeping the loss of power supply probability (LPSP) at zero level. The hourly energy output from these plants is then fed into MATLAB to determine the objective parameters for each case developed by the ANN. To train the ANN model to correctly predict the optimized system configuration, several training sets are required to feed the ANN model. A case study for this strategy has been implemented in Ras Ghareb, Egypt, which has had reliable measured data for over 20 years, for both solar and wind.

The remainder of the paper is organized as follows. System modeling and methodology is discussed in Section 2. Results and discussion of the proposed system are presented in Section 3. Finally, the conclusion of this work is presented in Section 4.

2. Modeling framework

As indicated in Figure 1, the proposed HRES comprises wind, PV cells, batteries and FCs. There are two power buses: a direct current (DC) bus for the battery system and hydrogen system, and an alternating current (AC) bus for the wind farm, PV plant and load. Energy is stored by using batteries and hydrogen chain devices. The Ras Ghareb site in the Gulf of Suez region was selected as a test site to conduct this analysis based on the following criteria: availability of wind and solar resources, and site constraints such as height and topography [39,41]. Figure 2 shows the whole model adopted in this study. It starts by preparing weather data for both wind and solar resources. This is followed by the modeling of renewable resources in order to get the hourly power generation profiles that will be fed into the load, along with the excess energy directed to the storage systems.

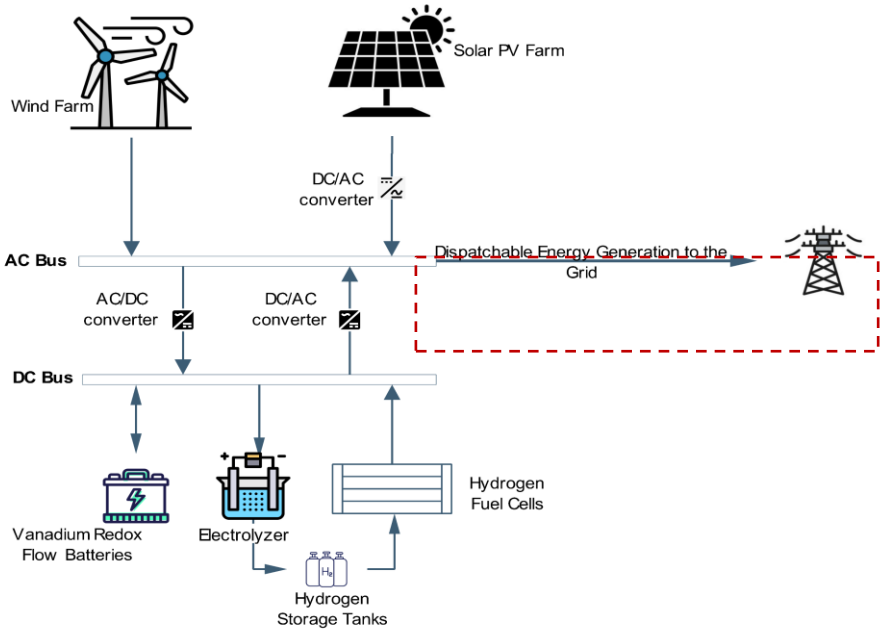

Figure 1. Proposed dispatchable HRES.

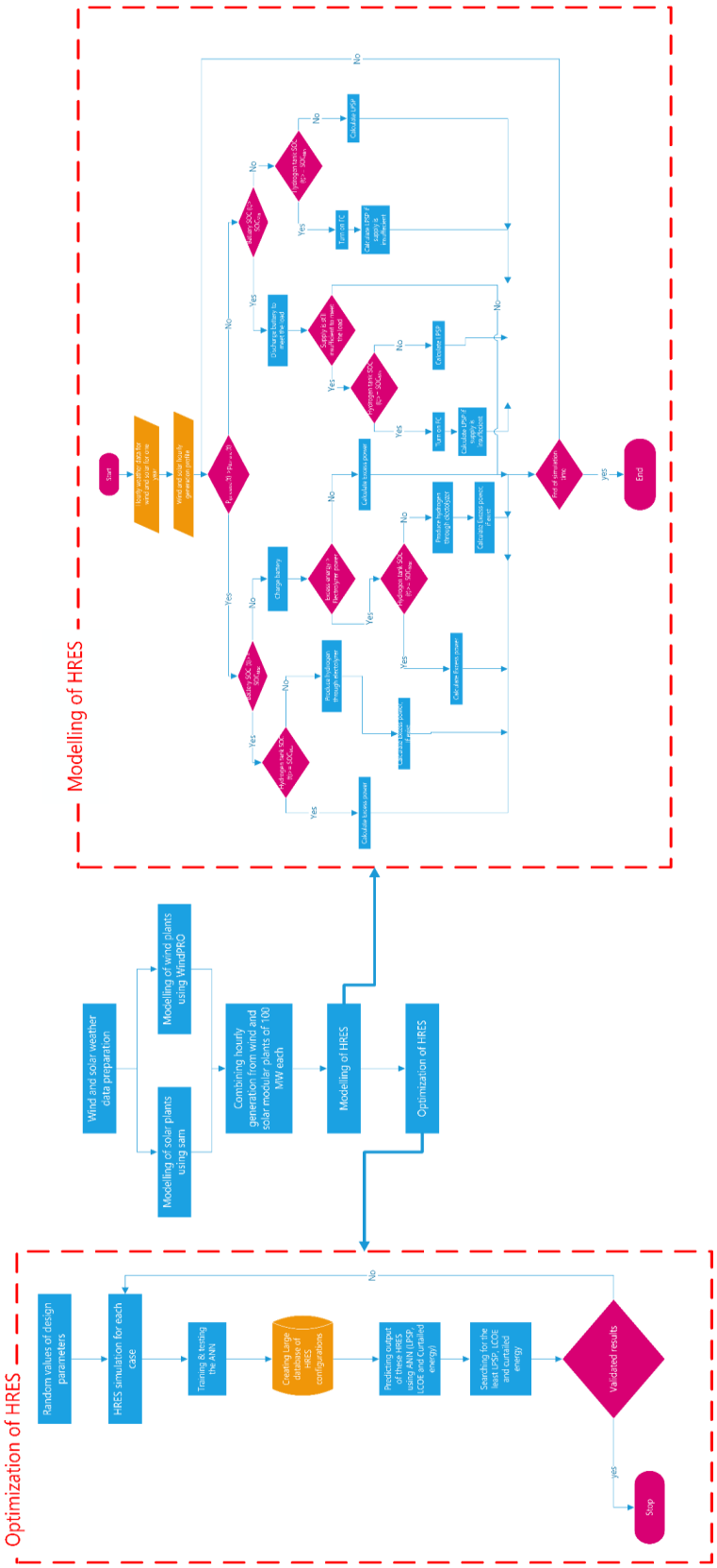

Figure 2. Proposed model framework.

2.1. Modeling and simulation of a wind system

Wind is the most intermittent renewable resource incorporated into the HRES. As a result, accurate weather data should be used to deliver reliable and acceptable outcomes. The Egyptian wind atlas and NREA [42] are used to collect reliable long-term weather statistics. Figure 3 shows the wind regime in Egypt, where the Gulf of Suez region is considered to have the greatest potential for wind power generation [42].

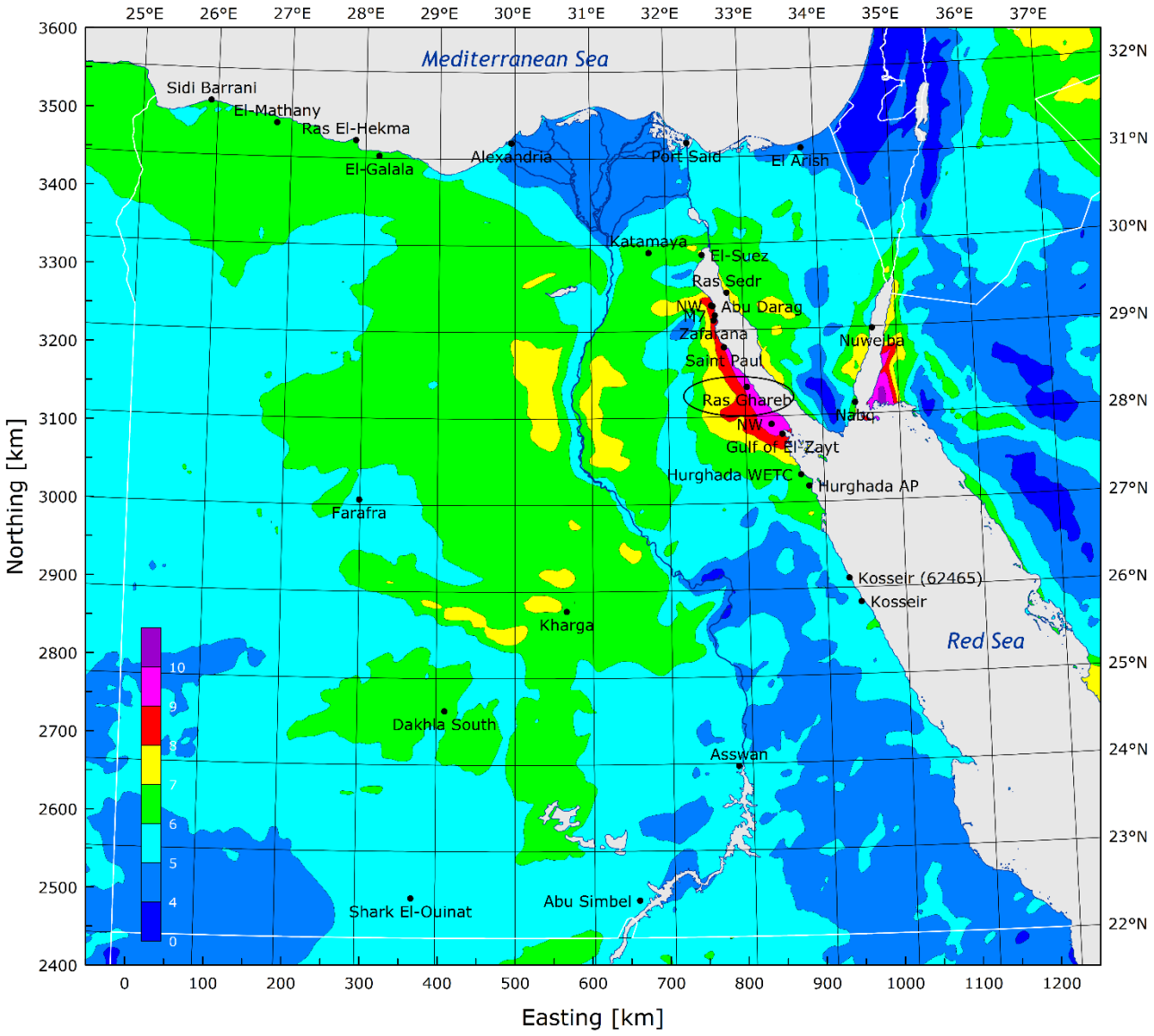

Figure 3. Wind speed map for Egypt at 24.5 m above ground level [42].

The average wind speed in Ras Ghareb is 9.5 s at 24.5 m above ground level. Figures 4 and 5 depict the average diurnal and seasonal wind speeds in Ras Ghareb, respectively. Ras Ghareb has a high wind potential all day, with high wind in summer and low wind in winter. As will be demonstrated later, the effect of this pattern will be visible in seasonal storage sizing and, hence, on the system cost (i.e., capital expenditure, CapEx).

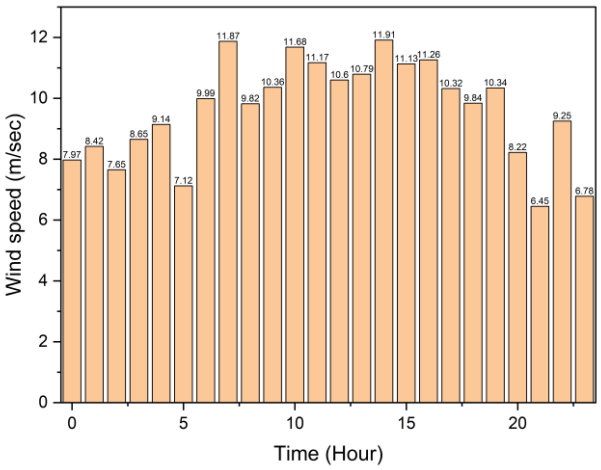

Figure 4. Average diurnal wind speed in Ras Ghareb.

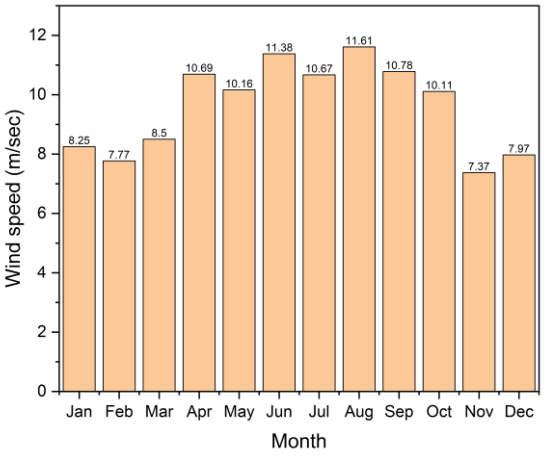

Figure 5. Average monthly wind speed in Ras Ghareb.

WindPRO software has been used to calculate the hourly generation from wind turbines. WindPRO is a professional software that can be used to conduct detailed wind energy studies such as hourly energy generation, wake losses, layout optimization, uncertainty analysis, environmental effect analysis and electrical and economic calculations [43]. On WindPRO, a modular plant with a capacity of 100 MW has been simulated and optimized in detail. The analysis considers the effects of land topography, ground coverage and wake losses. To get the highest capacity factor, optimization was carried out for the selection of the appropriate height and wind turbine and rotor diameters, yielding a performance curve that fits well with the wind pattern in the site. In addition, the optimal micro siting and intermediary distance between turbines have been defined to achieve minimal array losses. Table 3 lists the technical [43] and economic [44] characteristics employed in the investigation.

Table 3. Technical and economical parameters for wind plant [43,44].

Turbine rated power	2 MW	Installation cost	1100 $/kW (USD)
Hub height	80 m	O&M cost	67 $/kW/year (USD)
Turbine rotor diameter	100 m	Lifetime	25 years
Cut-in speed	3 m/s	Discount rate	9%
Cut-out speed	25 m/s		

2.2. Modeling and simulation of PV system

Solar PV energy is currently considered as one of the most cost-effective energy sources. PV energy is less intermittent and more predictable than wind; however, it has a zero capacity credit since Egypt's peak load occurs at night [45]. Egypt's solar PV potential is very high, particularly in the south, as illustrated in Figure 6 [46]. Weather data for the PV energy calculation were obtained from a PVGIS database [47]. Figure 7 shows the average monthly global horizontal irradiance (GHI) in Ras Ghareb.

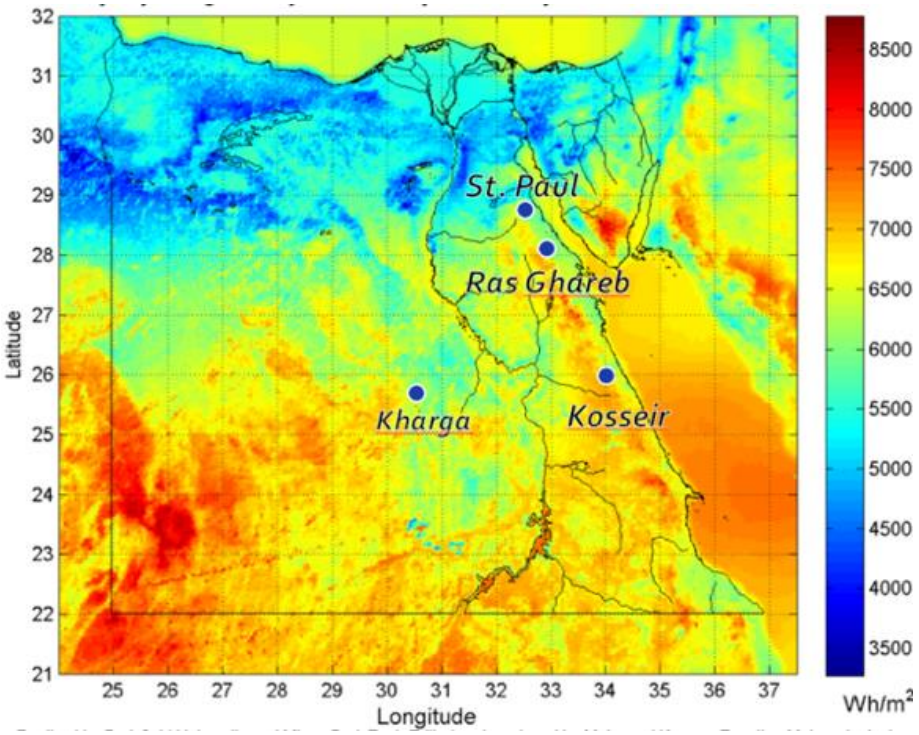

Figure 6. Global Horizontal Irradiance (GHI) for Egypt [46].

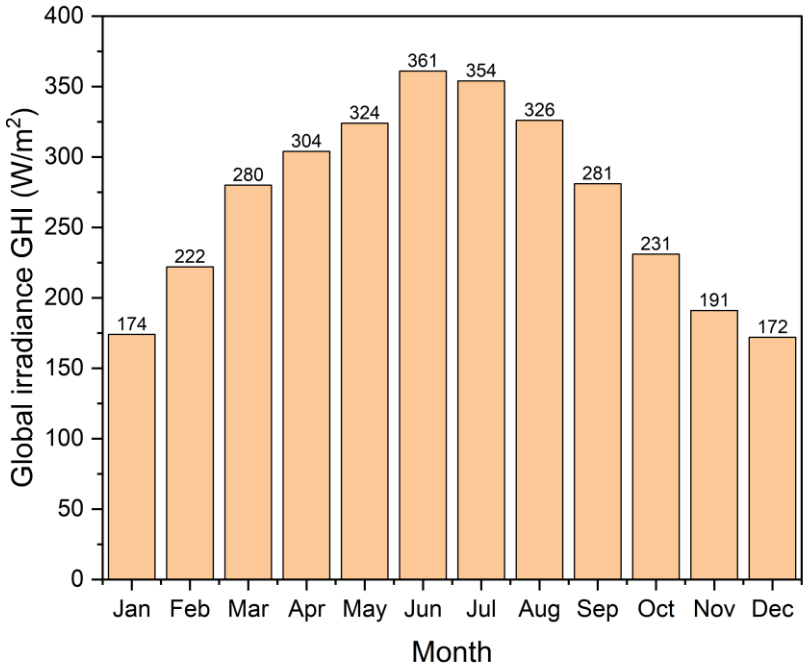

Figure 7. Average monthly GHI.

A SAM [48] was used to estimate the hourly generation from Ras Ghareb's modular 100-MW solar PV test plant. Table 4 lists the plant's technical and economic data. One-axis tracking was found to be a cost-effective approach after some initial cost optimization procedure. The DC-AC ratio and tilt angle were both adjusted for optimal performance and lowest LCOE.

Table 4. Technical and economical parameters for solar PV plant [44,48,49]

Module rated power	330 Watts	Installation cost	800 $/kW (USD)
DC-AC ratio	1.2	O&M cost	9 $/kW/year (USD)
Module tilt angle	29°	Lifetime	25 years
Inverter rated power DC	3.17 MW	Discount rate	9%
Tracking	1-axis (Azimuth)		

2.3. Battery system

A vanadium redox flow battery (VRFB) was employed in the analysis because of its long service life and timescale (charging and discharging in hours or days) [50]. VRFBs are distinct in that their power and energy ratings are independent [50]. VRFB energy is solely proportional to tank size; thus, saved energy can endure for days for any capacity. Curtailed wind and PV energy is used to charge the battery first, as shown in Eq (1).

$$E_b(t) = E_b(t-1) + \left(P_G(t) - P_{Load}(t)\right)\eta_b \quad (1)$$

where E_b is the battery energy, t is the time step over the year, P_G is the generated energy from renewables, P_{Load} is the required load energy provided to the grid and η_b is the battery efficiency.

When the demand is higher than the available power from wind and PV cells, the VRFB discharges the energy to satisfy the load as expressed in Eq (2).

$$E_b(t) = E_b(t-1) + \frac{P_G(t) - P_{Load}(t)}{\eta_b} \quad (2)$$

The technical and economical parameters for the VRFB are listed in Table 5. The storage capacity of the battery electrolyte tanks is limited by its state of charge: $SOC_{min} \leq SOC_{bat(t)} \leq SOC_{max}$.

Table 5. Technical and economical parameters for the VRFB [16,50–52].

Efficiency	85%	Installation cost	1152 $/kW (USD)
Max SOC	100%	O&M cost	50 $/kW (USD)
Min SOC	20%	Electrolyte cost	50 $/kWh (USD)
Number of cycles	12000 cycles	Life span	15 years

2.4. Green hydrogen system

Hydrogen as an energy vector has the potential to provide significant benefits in power networks with a high renewable penetration. It is a long-term (seasonal) energy storage system with a high energy density (lower heating value of 120 MJ/kg) [53–56]. The hydrogen system is made up of FCs, electrolyzers and hydrogen tanks, as well as other plant balance components such as a water desalination plant. Curtailed renewable energy from wind and PV cells is used to generate hydrogen, and gaseous hydrogen is then stored in hydrogen tanks. FCs convert hydrogen energy content into electricity and are utilized to supplement (stabilize) the HRES output delivered to the grid.

2.4.1. Electrolyzer

Water electrolyzers are classified based on their electrolyte, which might be alkaline, a proton exchange membrane (PEM) or a solid oxide electrolyzer. Because of their low dynamic responsiveness, alkaline electrolyzers are not appropriate for intermittent renewable resources. PEMs have a lot of potential because of its strong dynamic response and load ranges [57]. According to data from electrolysis manufacturers [58], the power usage for producing 1 kg of hydrogen is 51.8 kWh/kg of hydrogen. Hydrogen tanks will be utilized to store the hydrogen produced for later use in FCs.

2.4.2. FC

In this study, the battery system and the FC are operated sequentially or simultaneously. Priority is given to batteries because they have a better efficiency than the hydrogen system, and, hence, a lower energy cost. Equation (3) describes the modeling of the FC in the system.

$$P_{FC}(t) = H_{2used} \times 33.3 \frac{KWh}{Kg} \times \eta_{FC} \quad (3)$$

where P_{Fc} is the FC energy produced in this hour. Both the FC and electrolyzer technical and economical parameters are listed in Table 6.

Table 6. Hydrogen production and use specifications [59].

Electrolyzer efficiency	70%	FC efficiency	60%
Electrolyzer plant capital cost (including plant balance)	1000 $/kW (USD)	FC capital cost	1800 $/kW
Electrolyzer O&M cost	2% of CapEx	FC O&M cost	0.01 $/ Op.h
Electrolyzer lifetime	15 years	FC lifetime	50000 Op.h
Electrolyzer stack replacement cost	500 $/kW (USD)	FC replacement cost	1800 $/kW
Hydrogen storage cost	50 $/kg (USD)		

2.5. HRES sizing and optimization

2.5.1. Constraints

HRESs are always oversized to account for their intermittent production. Size optimization is usually required to compute the appropriate mix of technologies included in the hybrid system due to variance in the generating cost from individual system components. The goal is to minimize the LCOE while keeping the LPSP and curtailed energy at their minimum. These limits ensure that the system's reliability and cost objectives are met.

Consider that the objective function LCOE should be minimized. The LCOE is defined as the price at which electricity should be sold to break even at the end of the project lifetime, and it is calculated according to Eq (4).

$$LCOE = \frac{TC \times CRF + FOM}{AEP} \tag{4}$$

where *CRF* is the capital recovery factor, which is calculated as Eq (5).

$$CRF = \frac{D \times (1+D)^N}{(1+D)^N - 1} \tag{5}$$

where *D* is the discount rate, *N* is the lifetime of the project and *i* is the inflation rate.

The average annual discounted and inflated O&M (*FOM*) is calculated as Eq (6).

$$FOM = \frac{1}{N} \sum_{t=1}^{t=N} \frac{annualO\wedge M * D(1+i)^t}{(1+D)^t} \tag{6}$$

The concept of LPSP and curtailed energy are used in this paper to evaluate the reliability of the hybrid system. The LPSP is the probability of power shortage when the HRES is not able to satisfy the load. Curtailed energy is defined as the excess energy from the HRES when more power is generated than the load. Equations (7) and (8) show the methodology for calculating both constraints. Shortages and curtailed energy are calculated by summing the curtailed energy and energy shortage throughout the year.

$$LPSP = \frac{Shortage(MWh)}{HybridPlantMW} \times 8760 \tag{7}$$

$$CurtailedEnergy = \frac{CurtailedEnergy(MWh)}{HybridPlantMW} \times 8760 \tag{8}$$

2.5.2. Load profile

A variable load similar to the load pattern of Egypt was used in the analysis with a peak of 200 MW. Figure 8 shows the average diurnal load profile, and Figure 9 shows the yearly load profile.

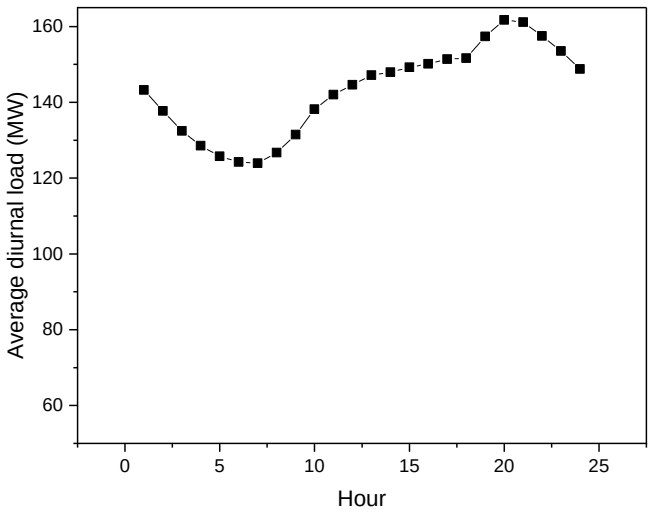

Figure 8. Average diurnal load during yearly analysis.

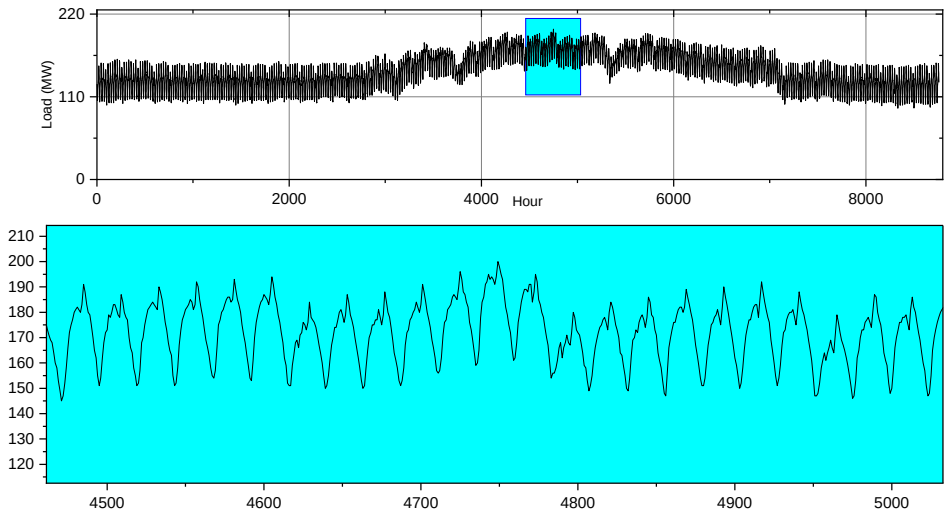

Figure 9. Annual load profile.

2.5.3. Modeling and optimization of HRES

Figure 2 depicts the steps of the sizing methodology, which was programmed in MATLAB. First, a set of system design parameters (seven design parameters) are chosen at random. These seven design parameters are as follows: wind plant capacity, PV plant capacity, VRFB capacity, VRFB energy, FC plant capacity, hydrogen electrolyzer capacity and hydrogen tank size. Wind plant capacity is used to

determine the hourly generation from wind energy by using WindPRO software, and PV plant capacity is used to determine the hourly generation from PV energy by using SAM software. Then, the code combines the hourly generation from solar and wind energies and compares them to the required dispatchable load. The code first tries to satisfy the required load with renewable energy, if the renewable energy generation is higher than the load, then the curtailed energy is stored in batteries and hydrogen tanks. If there is still renewable energy generation, it is considered as curtailed energy and should be curtailed. However, if the renewable energy generation is lower than the load, the VRFB operates first to fulfill the load, and then the FC operates if it is required. The LPSP increases if the load requirement is not fulfilled. The three outputs of this code are the LPSP, curtailed energy and LCOE. This process is repeated 3250 times by using different HRES configurations to form the training samples of the ANN model.

2.5.4. ANN

A feed-forward backpropagation learning algorithm was developed in MATLAB 2014 by using the neural network toolbox, and it is the neural network utilized in the investigation. The two layers of the ANN employed in the analysis are depicted in Figure 10. The hidden layer's number of neurons was tested and the least average mean square error was determined to be 15 neurons. So, the hidden layer has 15 neurons with the TANSIG transfer function, and the second layer is the output layer with the PURELIN transfer function. As previously mentioned, the analysis uses seven parameters as ANN inputs. The three outputs are curtailed energy, LPSP and LCOE. The training function used in the analysis is the Levenberg-Marquardt algorithm. A summary of the ANN model parameters is listed in Table 7.

Table 7. ANN parameters.

Network type	Feed-forward backpropagation	Neurons in the hidden layer	15
Input parameters	7	Transfer function	TANSIG
Output parameters	3	Training function	TRAINLM
No. of layers	2		

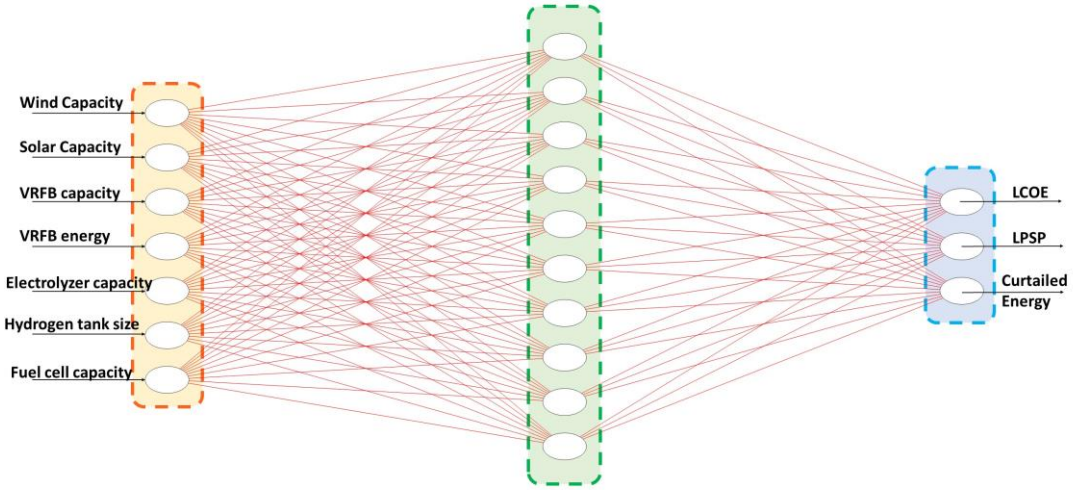

Figure 10. ANN structure.

Several HRES configurations (3250) are obtained via the method described in Figure 9 above. These data were divided into three categories, as follows: 70% of the samples were randomly chosen for training the ANN; 15% of the samples were randomly chosen to measure network generalization; 15% of the samples were randomly chosen to provide an independent measure of network performance during and after training.

The next stage involves constructing a huge dataset of HRES configurations after testing the ANN. The ANN model predicts the output of these systems; then, it limits the solution to target curtailed energy and LPSP values of 1% and 1%, respectively (see Figure 11 below). Limiting the solution to only 1% for the LPSP and curtailed energy serves to minimize the computational time. Figure 11 shows the complete algorithm; 9854220 HRES configurations were randomly created and fed into the ANN to predict its output.

3. Results

A grid-connected hybrid renewable energy plant was designed and optimized to supply the grid with a dispatchable generation regime according to the provided load profile, which is consistent with the load profile of Egypt. In order to ensure complementarity between solar and wind resources, the location was chosen based on the combined capacity factor for these two resources. The output parameters for several cases, which serve as a training dataset for the ANN, were determined by using a MATLAB code. A huge dataset that represents the space from which the best system is chosen based on the lowest LCOE within a range of established criteria for the LPSP and curtailed energy values is predicted by using an ANN.

3.1. Renewable energy results

The main output from the simulation of a modular wind plant is the hourly energy production, capacity factor and wake loss. Table 8 contains the main outputs for the 100-MW test wind plant.

Table 8. Main output for wind plant simulation.

Capacity factor	72%
Wake loss	4.3%
Total energy production for 100-MW plant	631.32 GWh/year

For the PV modular plant, the simulation's key outputs are the capacity factor and the hourly energy production. Table 9 shows the primary output of the PV system.

Table 9. Main outputs from solar PV plant.

Capacity factor	30.2%
AEP for 100-MW solar PV plant	264.9 GWh/year

3.2. ANN output

The regression curves in Figure 11 show the results of the network outputs of the target training, validation and testing, as obtained after training the network.

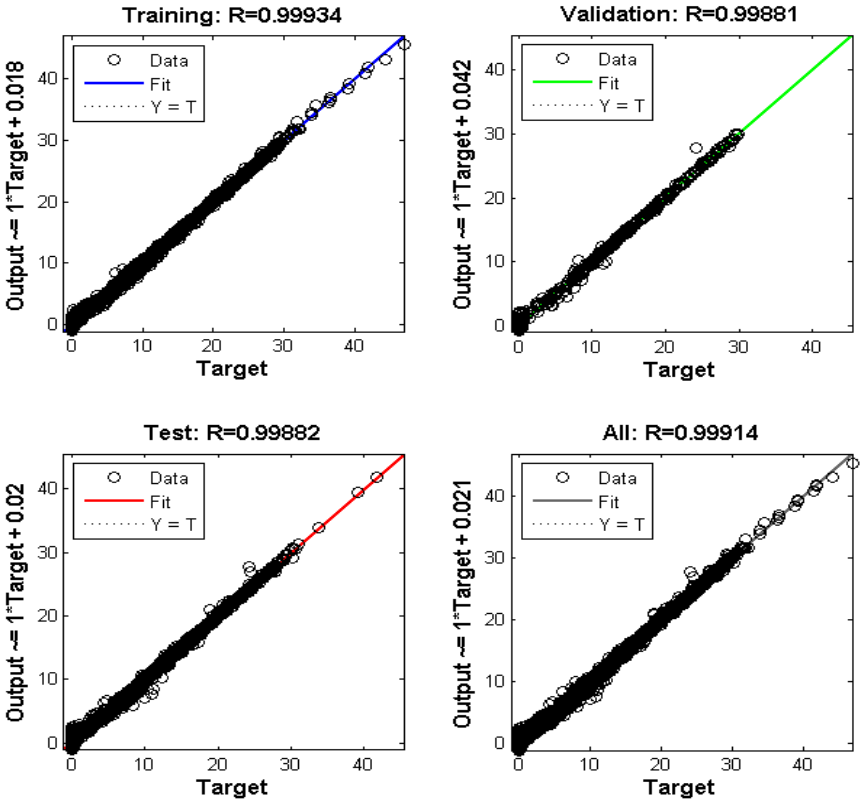

Figure 11. Regression analysis for sample data.

3.3. Base model results

The ANN sets a space of 9854220 HRES system configurations with three output parameters: LCOE, LPSP and curtailed energy. The lowest LCOE systems are most desired, but it comes with increases in the LPSP and curtailed energy. For the case presented here, we are focusing on zero LPSP and zero curtailed energy. Table 10 shows the optimum solution for the dispatchable generation plant.

Table 10. Optimum parameters for a dispatchable load HRES.

Parameter	Size
Wind energy	190-MW wind farm
Solar PV energy	90-MW solar PV farm
VRFB energy	2000 MWh
VRFB power	30 MW
Electrolyzer	150 MW
Hydrogen storage tanks	2300-ton H_2
FC	140 MW

The optimum solution should have zero LPSP and zero curtailed energy. Hence, the LCOE is only presented here because the two other constraints are zero. The LCOE for the above-mentioned plant is (USD) 9.3 cents/kWh.

Figures 12 and 13 show the energy share for each component of the HRES on a monthly and annual basis, respectively. As shown in the figures, renewable energy generation provides 91.3% of the total energy share, while 3.5% of the total energy share is from the VRFB and the remaining 5.2% is from hydrogen FCs. Wind energy share has the highest energy share due to the high-capacity factor of wind at that site.

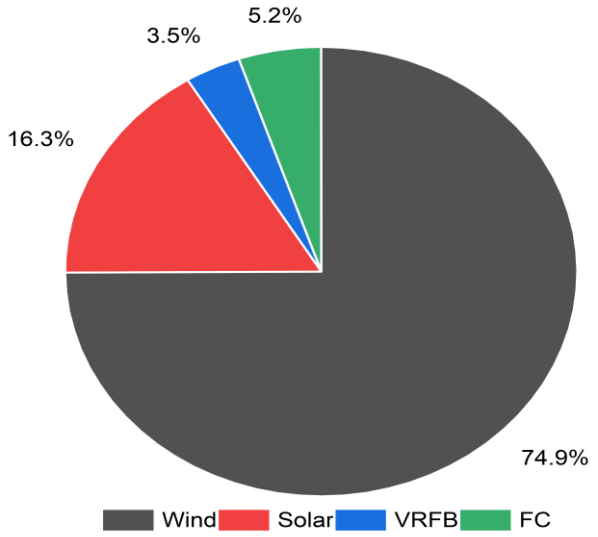

Figure 12. Annual energy share for each component.

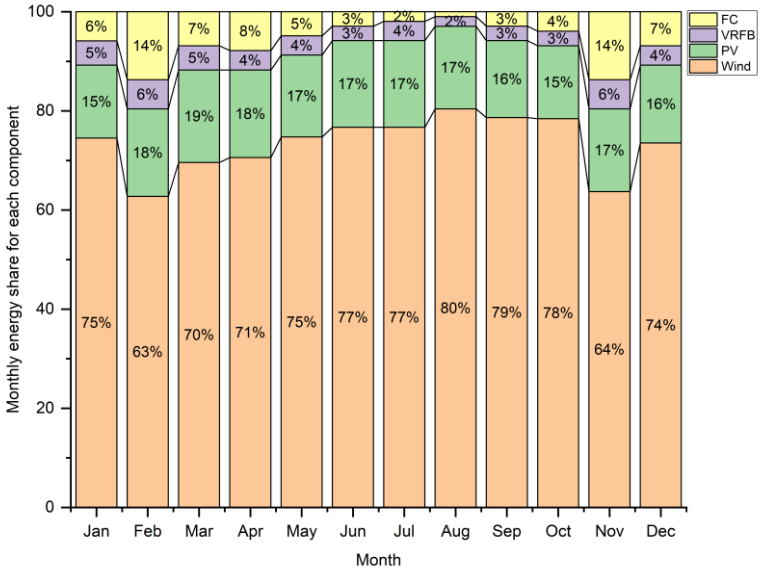

Figure 13. Monthly energy share for each component.

Figure 14 shows the variation in renewable energy production rates, the VRFB and hydrogen systems along on week in one sample week for the optimum HRES. The figure shows that wind and solar almost cover the required load in the daytime while it relies on storage systems in the night.

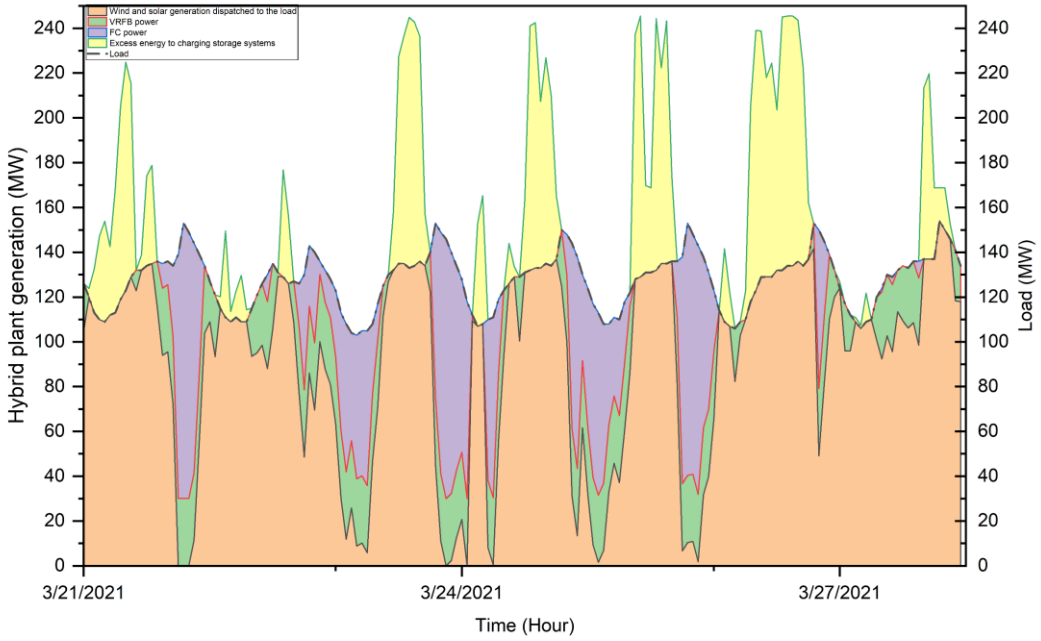

Figure 14. Hourly generation sample in one week.

Figure 15 shows the hourly generation for both the VRFB and FCs. The FCs will operate more during winter months, especially in February and November. However, due to the nature of the VRFB and its role as a diurnal storage system, it will operate more than FCs throughout the year.

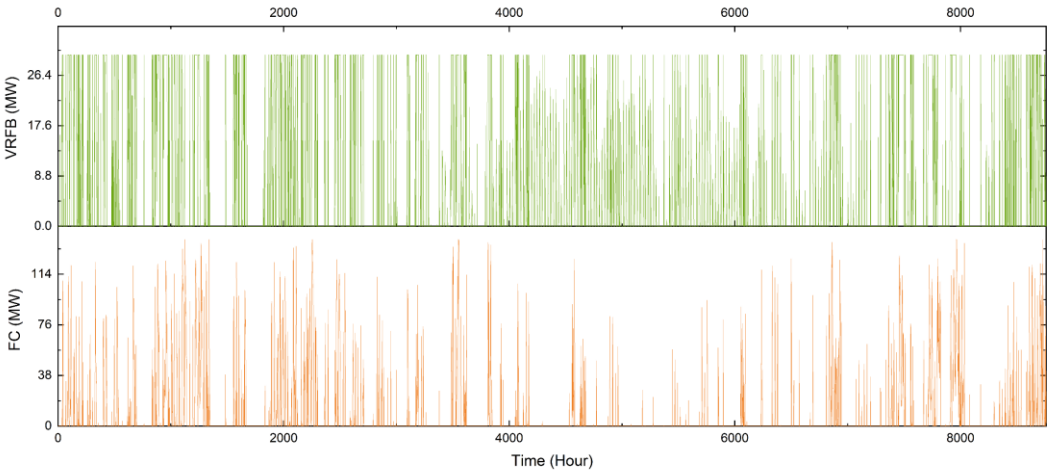

Figure 15. Energy generation for the VRFB and FCs.

Figure 16 presents the average monthly capacity factor. The monthly capacity factor for the VRFB will reach a maximum of 31.8% in November. For the FCs, the maximum monthly capacity factor of 16.2% will occur in February. The average yearly capacity factor for FCs is 6.8%, which is very low, because FCs operate as a seasonal storage system. On the other hand, the VRFB average yearly capacity factor is 21.25%.

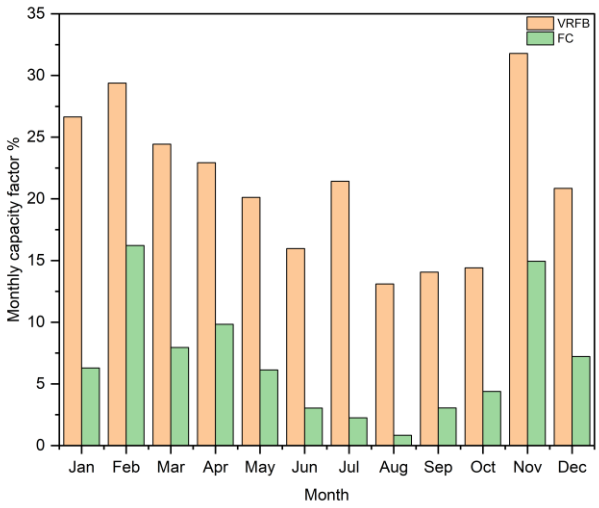

Figure 16. Average monthly capacity factor.

Batteries are more suitable for short-term storage. On the other hand, hydrogen storage is more suitable for seasonal storage. Figure 17 shows the annual variation in hydrogen storage level and the SOC of the VRFB. In the summer, the hydrogen level ramps up and accumulates for winter usage. This trend is consistent with the site's seasonal wind and solar patterns, where both wind and solar PV generation are higher in summer than in winter, as shown in Figures 5 and 6, respectively. The battery SOC shows the same trend as the hydrogen tank level. Despite the fact that the load profile is maximal during summer months, the storage requirement is maximal in winter months. This is directly related to the nature of the wind speed at the studied site, because the wind speed is low in winter months. It is obvious that the system depends on storage more than the renewable generation to provide a steady output for the winter period. However, the VRFB will cycle more than hydrogen due to its shorter storage period (less than a week). Therefore, the system depends on the seasonal storage of hydrogen more than on battery storage.

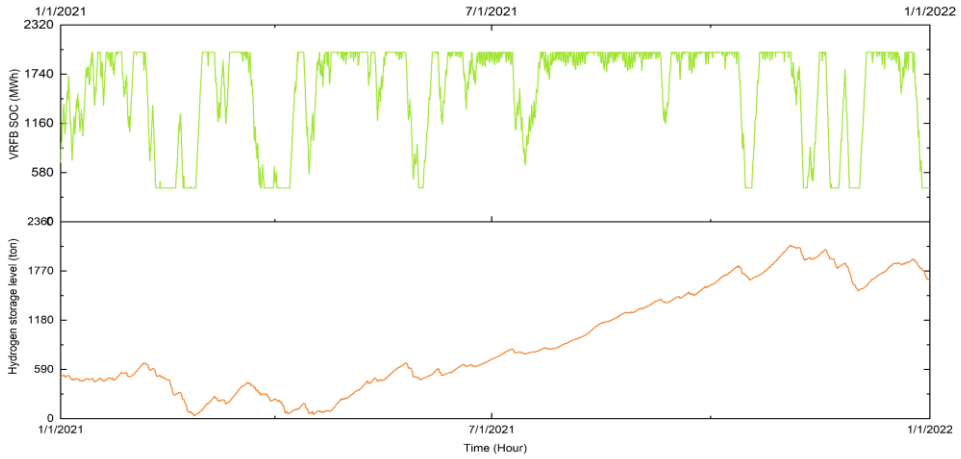

Figure 17. Hydrogen storage level and VRFB SOC.

Introducing energy storage systems to a hybrid plant increases the system reliability and reduces the intermittency, enabling a steady output. However, it substantially increases the cost of the system and, hence, the LCOE, due to its higher CapEx. Figure 18 shows the breakdown of the total CapEx of the HRES and its percentage of total plant cost. The total system CapEx is projected to be USD 0.947 billion, which means that the cost per kilowatt is USD 4735.

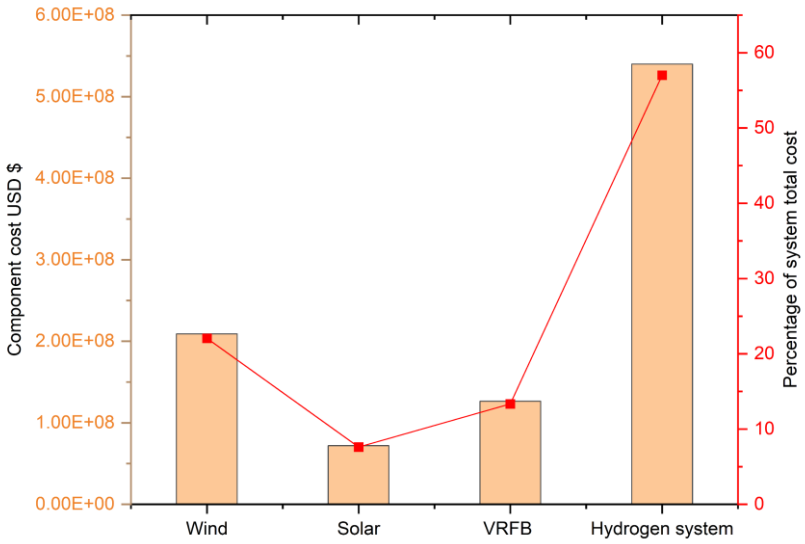

Figure 18. Breakdown of HRES CapEx.

Hydrogen itself is responsible for 57% of the total plant cost, despite the low-capacity factor of the FCs. But it is important to improve the system reliability and flexibility.

The installation cost of wind and solar PV plants represent 30% of the total system cost. And, they are responsible for 91.2% of the total energy share. On the other hand, the energy storage system cost represents 70% of the total system cost and produces only 8.8% of the total energy share. A substantial initial cost is one of the obstacles preventing the wide adoption of such systems. However, as technology advances and economies of scale take hold, storage costs will continue to decline, gradually closing the gap.

3.4. Relaxing constraints

The base case model considers LPSP and curtailed energy to be zero. However, relaxing the curtailed energy parameter could reduce the LCOE while keeping the LPSP at zero. This is because an oversized renewable generation plant will reduce the required storage and, hence, increase the curtailed energy. Figure 19 shows the case of relaxing the curtailed energy constraint from 0% to 10%. It shows a reduction of 14.5% of the LCOE when the curtailed energy is 10%.

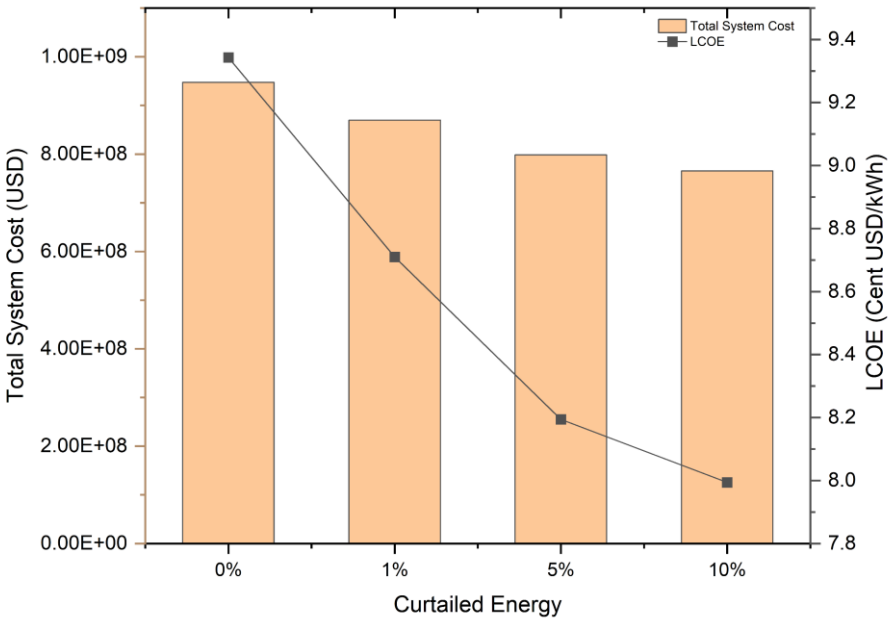

Figure 19. Effects of relaxing curtailed energy constraint on the system cost and LCOE.

4. Conclusions

Although the plant consists of several renewable and storage systems, including wind turbines, PV cells, a VRFB and hydrogen systems, it is possible to optimally consolidate them into one plant, which can be operated on a dispatchable mode. The plant enjoys a fast response time due to the presence of batteries. The optimum LCOE is a function of the site characteristics and load profile. Testing the model, considering Egypt's load profile at the site of Ras Ghareb in the Gulf of Suez in Egypt, the LCOE is projected to be (USD) 9.3 ¢/kWh at zero LPSP. Although this cost may not achieve grid parity, it can be economical if the international gas prices and greenhouse gas emission abatement costs are considered. Furthermore, this cost is less than an equivalent concentrated solar power plant with thermal storage. Relaxing the constraint of curtailed energy while keep the LPSP at zero can have an obvious impact on the cost of the generated electricity. The storage system is responsible for 70% of the cost of electricity. This can be reduced substantially for sites that have better coupling (i.e., negative cross-correlation between the generation of both solar and wind) and good coupling with the annual load profile (i.e., positive cross-correlation, especially for wind energy generation and the load profile).

Conflict of interest

The authors declare no conflict of interest.

References

1. Akuru UB, Onukwube IE, Okoro OI, et al. (2017) Towards 100% renewable energy in Nigeria. *Renewable Sustainable Energy Rev* 71: 943–953. https://doi.org/10.1016/j.rser.2016.12.123
2. Kiwan S, Al-Gharibeh E (2020) Jordan toward a 100% renewable electricity system. *Renewable Energy* 147: 423–436. https://doi.org/10.1016/j.renene.2019.09.004
3. Hansen K, Mathiesen BV, Skov IR (2019) Full energy system transition towards 100% renewable energy in Germany in 2050. *Renewable Sustainable Energy Rev* 102: 1–13. https://doi.org/10.1016/j.rser.2018.11.038
4. Zappa W, Junginger M, van den Broek M (2019) Is a 100% renewable European power system feasible by 2050? *Appl Energy* 233–234: 1027–1050. https://doi.org/10.1016/j.apenergy.2018.08.109
5. International Energy Agency (2022) Renewable Energy Market Update. https://doi.org/10.1787/faf30e5a-en
6. IEA (2019) Data tables—Data & Statistics. Available from: https://www.iea.org/data-and-statistics/data-tables/?country=WORLD&energy=Electricity&year=2019.
7. Welsch M, Deane P, Howells M, et al. (2014) Incorporating flexibility requirements into long-term energy system models—A case study on high levels of renewable electricity penetration in Ireland. *Appl Energy* 135: 600–615. https://doi.org/10.1016/j.apenergy.2014.08.072
8. Panagiotakopoulou P (2012) Analysing the effects of future generation and grid investments on the Spanish power market, with large scale wind integration, using PLEXOS ® for Power. 11th Wind Integr Work.
9. Steurer M, Fahl U, Voß A, et al. (2017) Curtailment: An option for cost-efficient integration of variable renewable generation? *Eur Energy Transit*, 97–104. https://doi.org/10.1016/B978-0-12-809806-6.00015-8
10. Van Den Bergh K, Delarue E (2015) Cycling of conventional power plants: Technical limits and actual costs. *Energy Convers Manage* 97: 70–77. https://doi.org/10.1016/j.enconman.2015.03.026
11. Bizon N, Oproescu M, Raceanu M (2015) Efficient energy control strategies for a standalone renewable/fuel cell hybrid power source. *Energy Convers Manage* 90. https://doi.org/10.1016/j.enconman.2014.11.002
12. Aziz AS, Tajuddin MFN, Adzman MR, et al. (2019) Energy management and optimization of a PV/diesel/battery hybrid energy system using a combined dispatch strategy. *Sustainability* 11: 683. https://doi.org/10.3390/su11030683
13. Pérez-Navarro A, Alfonso D, Ariza HE, et al. (2016) Experimental verification of hybrid renewable systems as feasible energy sources. *Renewable Energy* 86: 384–391. https://doi.org/10.1016/j.renene.2015.08.030
14. Al-Ghussain L, Ahmed H, Haneef F (2018) Optimization of hybrid PV-wind system: Case study Al-Tafilah cement factory, Jordan. *Sustainable Energy Technol Assess* 30: 24–36. https://doi.org/10.1016/j.seta.2018.08.008
15. Samy MM, Emam A, Tag-Eldin E, et al. (2022) Exploring energy storage methods for grid-connected clean power plants in case of repetitive outages. *J Energy Storage* 54: 105307. https://doi.org/10.1016/j.est.2022.105307

16. Yang Y, Menictas C, Bremner S, et al. (2018) A Comparison study of dispatching various battery technologies in a hybrid PV and wind power plant. *2018 IEEE Power & Energy Society General Meeting (PESGM),* 1–5. https://doi.org/10.1109/PESGM.2018.8585803
17. Fathima H, Palanisamy K (2015) Optimized sizing, selection, and economic analysis of battery energy storage for grid-connected wind-PV hybrid system. *Model Simul Eng* 2015: 1–16. https://doi.org/10.1155/2015/713530
18. Ghorbani N, Kasaeian A, Toopshekan A, et al. (2017) Optimizing a hybrid wind-PV-battery system using GA-PSO and MOPSO for reducing cost and increasing reliability. *Energy* 154: 581–591. https://doi.org/10.1016/j.energy.2017.12.057
19. Cano A, Jurado F, Sánchez H, et al. (2014) Optimal sizing of stand-alone hybrid systems based on PV/WT/FC by using several methodologies. *J Energy Inst* 87: 330–340. https://doi.org/10.1016/j.joei.2014.03.028
20. Ceran B (2019) The concept of use of PV/WT/FC hybrid power generation system for smoothing the energy profile of the consumer. *Energy* 167: 853–865. https://doi.org/10.1016/j.energy.2018.11.028
21. Nasiraghdam H, Jadid S (2012) Optimal hybrid PV/WT/FC sizing and distribution system reconfiguration using multi-objective artificial bee colony (MOABC) algorithm. *Sol Ener*gy 86: 3057–3071. https://doi.org/10.1016/j.solener.2012.07.014
22. Das HS, Tan CW, Yatim AHM, et al. (2017) Feasibility analysis of hybrid photovoltaic/battery/fuel cell energy system for an indigenous residence in East Malaysia. *Renewable Sustainable Energy Re*v 76: 1332–1347. https://doi.org/10.1016/j.rser.2017.01.174
23. Zurita A, Mata-Torres C, Valenzuela C, et al. (2018) Techno-economic evaluation of a hybrid CSP + PV plant integrated with thermal energy storage and a large-scale battery energy storage system for base generation. *Sol Energy* 173: 1262–1277. https://doi.org/10.1016/j.solener.2018.08.061
24. Hosseinalizadeh R, Shakouri G H, Amalnick MS, et al. (2016) Economic sizing of a hybrid (PV-WT-FC) renewable energy system (HRES) for stand-alone usages by an optimization-simulation model: Case study of Iran. *Renewable Sustainable Energy R*ev 54: 139–150. https://doi.org/10.1016/j.rser.2015.09.046
25. Jing W, Lai CH, Wong WSH, et al. (2018) A comprehensive study of battery-supercapacitor hybrid energy storage system for standalone PV power system in rural electrification. *Appl Energy* 224: 340–356. https://doi.org/10.1016/j.apenergy.2018.04.106
26. Luta DN, Raji AK (2019) Optimal sizing of hybrid fuel cell-supercapacitor storage system for off-grid renewable applications. *Energy* 166: 530–540. https://doi.org/10.1016/j.energy.2018.10.070
27. Wu T, Zhang H, Shang L (2020) Optimal sizing of a grid-connected hybrid renewable energy systems considering hydroelectric storage. *Energy Sources, Part A: Recover Util Environ Eff.* https://doi.org/10.1080/15567036.2020.1731018
28. Heydari A, Askarzadeh A (2016) Techno-economic analysis of a PV/biomass/fuel cell energy system considering different fuel cell system initial capital costs. *Sol Ener*gy 133: 409–420. https://doi.org/10.1016/j.solener.2016.04.018
29. Halabi LM, Mekhilef S, Olatomiwa L, et al. (2017) Performance analysis of hybrid PV/diesel/battery system using HOMER: A case study Sabah, Malaysia. *Energy Convers Manage* 144: 322–339. https://doi.org/10.1016/j.enconman.2017.04.070

30. Lau KY, Yousof MFM, Arshad SNM, et al. (2010) Performance analysis of hybrid photovoltaic/diesel energy system under Malaysian conditions. *Energy* 35: 3245–3255. https://doi.org/10.1016/j.energy.2010.04.008
31. Javed MS, Song A, Ma T (2019) Techno-economic assessment of a stand-alone hybrid solar-wind-battery system for a remote island using genetic algorithm. *Energy* 176: 704–717. https://doi.org/10.1016/j.energy.2019.03.131
32. Nagapurkar P, Smith JD (2019) Techno-economic optimization and environmental life cycle assessment (LCA) of microgrids located in the US using genetic algorithm. *Energy Convers Manag*e 181: 272–291. https://doi.org/10.1016/j.enconman.2018.11.072
33. Tabanjat A, Becherif M, Hissel D, et al. (2018) Energy management hypothesis for hybrid power system of H2/WT/PV/GMT via AI techniques. *Int J Hydrogen Energy* 43: 3527–3541. https://doi.org/10.1016/j.ijhydene.2017.06.085
34. Patel AM, Singal SK (2019) Optimal component selection of integrated renewable energy system for power generation in stand-alone applications. *Energy* 175: 481–504. https://doi.org/10.1016/j.energy.2019.03.055
35. Dhundhara S, Verma YP, Williams A (2018) Techno-economic analysis of the lithium-ion and lead-acid battery in microgrid systems. *Energy Convers Manage* 177: 122–142. https://doi.org/10.1016/j.enconman.2018.09.030
36. Zhang W, Maleki A, Rosen MA, et al. (2018) Optimization with a simulated annealing algorithm of a hybrid system for renewable energy including battery and hydrogen storage. *Energy* 163: 191–207. https://doi.org/10.1016/j.energy.2018.08.112
37. Brekken TKA, Yokochi A, Von Jouanne A, et al. (2011) Optimal energy storage sizing and control for wind power applications. *IEEE Trans Sustainable Energy* 2: 69–77. https://doi.org/10.1109/TSTE.2010.2066294
38. Zhang W, Maleki A, Rosen MA, et al. (2019) Sizing a stand-alone solar-wind-hydrogen energy system using weather forecasting and a hybrid search optimization algorithm. *Energy Convers Manag*e 180: 609–621. https://doi.org/10.1016/j.enconman.2018.08.102
39. Hamdi M, Ragab R, El Salmawy HA (2023) The value of diurnal and seasonal energy storage in baseload renewable energy systems: A case study of Ras Ghareb-Egypt. *J Energy Storage* 61: 106764. https://doi.org/10.1016/j.est.2023.106764
40. Rahman MM, Shakeri M, Tiong SK, et al. (2021) Prospective methodologies in hybrid renewable energy systems for energy prediction using artificial neural networks. *Sustainability* 13: 1–28. https://doi.org/10.3390/su13042393
41. Ragab R, Hamdi M, Al ST, et al. (2021) Optimized hybrid renewable energy system for a baseload plant. *Appl Energy Symp.*
42. Mortensen, NG, Hansen JC, Badger J, et al. (2005) Wind Atlas for Egypt, measurements and modelling. 1991–2005.
43. EMD International, windPRO. Available from: https://www.emd-international.com/windpro/.
44. Renewable power generation costs in 2020. Available from: https://www.irena.org/publications/2021/Jun/Renewable-Power-Costs-in-2020.
45. Egyptian electricity holding company (2020) Annual report of the Egyptian electricity holding company2019/2020.
46. Goyena R, Fallis A (2019) Solar atlas of Egypt.

47. EU Science Hub. Photovoltaic Geographical Information System (PVGIS). Available from: https://ec.europa.eu/jrc/en/pvgis.
48. Home-System Advisor Model (SAM). Available from: https://sam.nrel.gov/.
49. Home Page-New and Renewable Energy Authoroty. Available from: http://www.nrea.gov.eg/.
50. Guarnieri M, Mattavelli P, Petrone G, et al. (2016) Vanadium redox flow batteries: Potentials and challenges of an emerging storage technology. *IEEE Ind Electron Mag* 10: 20–31. https://doi.org/10.1109/MIE.2016.2611760
51. Castillo A, Gayme DF (2014) Grid-scale energy storage applications in renewable energy integration: A survey. *Energy Convers Manage* 87: 885–894. https://doi.org/10.1016/j.enconman.2014.07.063
52. IRENA (2017) Electricity storage and renewables: Costs and markets to 2030.
53. Abdalla AM, Hossain S, Nisfindy OB, et al. (2018) Hydrogen production, storage, transportation and key challenges with applications: A review. *Energy Convers Manage* 165: 602–627. https://doi.org/10.1016/j.enconman.2018.03.088
54. Abe JO, Popoola API, Ajenifuja E, et al. (2019) Hydrogen energy, economy and storage: Review and recommendation. *Int J Hydrogen Energy* 44: 15072–15086. https://doi.org/10.1016/j.ijhydene.2019.04.068
55. Moradi R, Groth KM (2019) Hydrogen storage and delivery: Review of the state of the art technologies and risk and reliability analysis. *Int J Hydrogen Energy* 44: 12254–12269. https://doi.org/10.1016/j.ijhydene.2019.03.041
56. Gahleitner G (2012) Hydrogen from renewable electricity: An international review of power-to-gas pilot plants for stationary applications. *Int J Hydrogen Energy* 38: 2039–2061. https://doi.org/10.1016/j.ijhydene.2012.12.010
57. El-Emam RS, Özcan H (2019) Comprehensive review on the techno-economics of sustainable large-scale clean hydrogen production. *J Clean Prod* 220: 593–609. https://doi.org/10.1016/j.jclepro.2019.01.309
58. Siemens Energy—Benefits of green hydrogen. Available from: https://www.siemens-energy.com/global/en/offerings/renewable-energy/hydrogen-solutions.html.
59. IRENA (2020) Green hydrogen cost reduction.